Novel stable compounds in the Mg–O system under high pressure†

Qiang Zhu,*[a] Artem R. Oganov[ab] and Andriy O. Lyakhov[a]

Using *ab initio* evolutionary simulations, we explore the entire range of possible stoichiometries for the Mg–O system at pressures of up to 850 GPa. In addition to MgO, our calculations find that two extraordinary compounds MgO_2 and Mg_3O_2 become thermodynamically stable at 116 GPa and 500 GPa, respectively. Detailed chemical bonding analysis shows large charge transfer in all magnesium oxides. MgO_2 contains peroxide ions $[O–O]^{2-}$, while non-nuclear electron density maxima play the role of anions in the electride compound Mg_3O_2. The latter compound is calculated to have a much narrower band gap compared to MgO and MgO_2. We discuss the conditions under which MgO_2 and Mg_3O_2 could exist in planetary interiors.

1 Introduction

Magnesium oxide (MgO) is one of the most abundant phases in planetary mantles, and understanding its high-pressure behavior is essential for constructing models of the Earth and planetary interiors. For a long time, MgO was believed to be among the least polymorphic solids – only the NaCl-type structure has been observed in experiments at pressures of up to 227 GPa.[1] Static theoretical calculations have proposed that the NaCl-type (B1) MgO would transform into the CsCl-type (B2) and the transition pressure is approximately 490 GPa at 0 K (474 GPa with the inclusion of zero-point vibration).[2–4] Calculations also predicted that MgO remains non-metallic up to extremely high pressure (20.7 TPa),[3,5] making it to our knowledge the most difficult mineral to metalize. Thermodynamic equilibria in the Mg–O system at 0.1 MPa pressure have been summarized in previous studies,[6–8] concluding that only MgO is a stable composition, though metastable compounds (MgO_2, MgO_4) can be prepared at very high oxygen fugacities.

Although MgO seems to be so simple and well understood, surprises may be in store for the researcher. For instance, it was recently predicted that Xe becomes reactive and forms thermodynamically stable oxides at pressures of the Earth's mantle.[9] In the "simple" Li–H system, in addition to the "normal" LiH, new counterintuitive compounds LiH_2, LiH_6 and LiH_8 were predicted to become stable at pressures above 100 GPa,[10] though experiments

failed to confirm them so far.[11] However, the prediction of new Na–Cl compounds (Na_3Cl, Na_2Cl, Na_3Cl_2, $NaCl_3$ and $NaCl_7$) has been confirmed by the experiment.[12] If similarly unusual stoichiometries become stable also in the Mg–O system, this could have important chemical and planetological implications. In this paper, we explore this possibility and indeed find two new stoichiometries to be thermodynamically stable at high pressures. These two new stable compounds (MgO_2 and Mg_3O_2) exhibit interesting crystal structures with unusual chemical bonding and insulating and semiconducting electronic structures, respectively.

2 Methods

Searches for the stable compounds and structures were performed using an evolutionary algorithm, as implemented in the USPEX code.[13–15] The most significant feature of USPEX we used in this work is the capability of searching for a specific area of the composition space – as opposed to the more usual structure predictions at fixed chemical composition. The desired composition space is described *via* building blocks (for example, search for all compositions in a form of $[xAl_2O_3 + yMgO]$ or $[xMg + yO]$). During the initialization, USPEX samples the whole range of compositions of interest randomly and sparsely. Chemistry-preserving constraints in the variation operators are lifted and replaced by the block-correction scheme which ensures that a child structure is within the desired area of compositional space, and a new "chemical transmutation" operator is introduced.[16] Stable compositions are determined using the convex hull construction: a compound is thermodynamically stable if the enthalpy of its decomposition into any other compounds is positive. Structure prediction was done in conjunction with *ab initio* structure relaxations based on

[a] Department of Geosciences, Department of Physics and Astronomy, Stony Brook University, Stony Brook, New York 11794, USA.
E-mail: qiang.zhu@stonybrook.edu; Fax: +1 631 632 8240; Tel: +1 631 632 1449
[b] Geology Department, Moscow State University, Moscow 119992, Russia
† Electronic supplementary information (ESI) available. See DOI: 10.1039/c3cp50678a

7696 | *Phys. Chem. Chem. Phys.*, 2013, **15**, 7696–7700

This journal is © the Owner Societies 2013

density functional theory (DFT) within the Perdew–Burke–Ernzerhof (PBE) generalized gradient approximation (GGA),[17] as implemented in the VASP code.[18] For structural relaxation, we used the all-electron projector-augmented wave (PAW) method[19] and the plane wave basis set with the 600 eV kinetic energy cutoff; the Brillouin zone was sampled by Monkhorst–Pack meshes with the resolution $2\pi \times 0.06$ Å^{-1}. Such calculations provide an excellent description of the known structures (Mg, O_2, MgO) and their energetics. To ensure that the obtained structures are dynamically stable, we calculated phonon frequencies throughout the Brillouin zone using the finite-displacement approach as implemented in the Phonopy code.[20] Phonon calculations also allowed us to explore the effects of temperature within the quasiharmonic approximation; for each structure, phonons were calculated at 10–15 different volumes.

3 Thermodynamically stable compounds in the Mg–O system

We have performed structure searches with up to 20 atoms in the unit cell at pressures in the range of 0–850 GPa for the Mg–O system. These searches yielded MgO as a stable oxide, but additionally two new compounds were predicted to be stable in the regions of high and low oxygen chemical potential, respectively. To confirm this and to obtain the most accurate results, we then focused search on two separate regions of chemical space; Mg–MgO and MgO–O, respectively. Since the structures in the two regions exhibit different properties, we report them separately.

3.1 Exploring phase stability at high oxygen fugacities: the MgO–O system and stable peroxide MgO_2

It is well known that monovalent (H–Cs) and divalent (Be–Ba and Zn–Hg) elements are able to form not only normal oxides, but also peroxides and even superoxides[21] (for instance, BaO_2 has been well studied at both ambient and high pressure[22,23]). Fig. 1 shows the calculated thermodynamics of the Mg–MgO
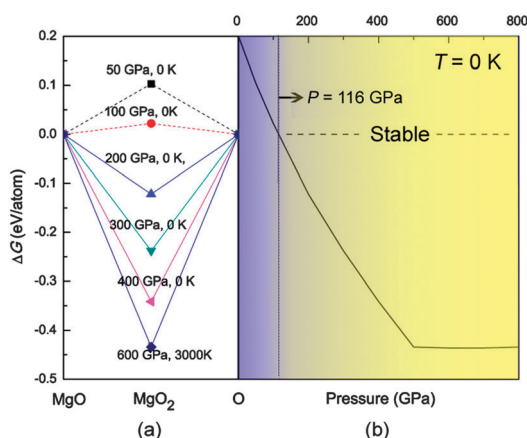

Fig. 1 (a) Convex hull for the MgO–O system at high pressures; (b) the enthalpy of formation of MgO_2 as a function of pressure. For oxygen, we used the earlier predicted structures.[25] For MgO, B1 and B2 phases were considered. c-MgO_2 was considered below 50 GPa, while t-MgO_2 was used at pressures higher than 50 GPa.
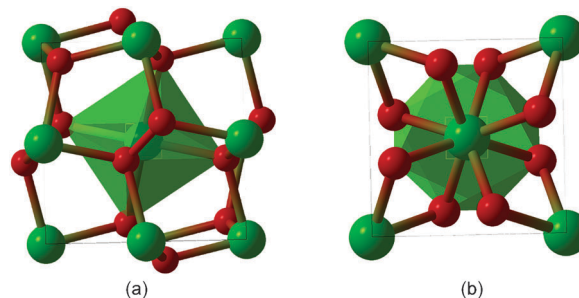

Fig. 2 Crystal structures of (a) c-MgO_2 phase at 50 GPa, space group $Pa3$, a = 4.524 Å, Mg(0, 0, 0), O(0.4074, 0.4074, 0.4074); (b) t-MgO_2 at 500 GPa, space group $I4/mcm$, a = 3.377 Å, c = 3.985 Å, Mg(0, 0, 0.75), O(0.1260, 0.3740, 0.5). The green polyhedra are drawn to show the coordination environment of Mg atoms (6-fold in c-MgO_2, and 8-fold in t-MgO_2).

system, indicating thermodynamic stability of MgO_2. Our structure prediction calculations identified the presence of magnesium peroxide with $Pa3$ symmetry and 12 atoms in the unit cell at ambient pressure, which is in good agreement with experimental results.[24] In this cubic phase, Mg is octahedrally coordinated by oxygen atoms (which form O_2 dumbbells), see Fig. 2a. However, $Pa3$ MgO_2 (c-MgO_2 from now on) is calculated to have a positive formation enthalpy from Mg and O_2, and is therefore metastable. The calculation shows that upon increasing pressure, c-MgO_2 transforms into a tetragonal form with the space group $I4/mcm$. In the t-MgO_2 phase (Fig. 2b), Mg is 8-coordinate. Here we see the same trend of change from 6-fold to 8-fold coordination as in the predicted B1–B2 transition in MgO, but in MgO_2 it happens at mere 53 GPa, compared to 490 GPa for MgO. Most remarkably, above 116 GPa the t-MgO_2 structure has a negative enthalpy of formation from MgO and O_2, indicating that t-MgO_2 becomes thermodynamically stable. Furthermore, its stability is greatly enhanced by pressure and its enthalpy of formation becomes impressively negative, -0.43 eV per atom, at 500 GPa! We also examined the effect of temperature on its stability by performing quasiharmonic free energy calculations. Thermal effects tend to decrease the relative stability of MgO_2 by 0.008 meV atom^{-1} K, which is clearly insufficient to change the sign of the free energy of formation (ΔG), and MgO_2 remains stable at high temperatures.

3.2 Phase diagram of the Mg–MgO system: Mg_3O_2 is an exotic stable compound

For the Mg-rich part of the Mg–O phase diagram, USPEX shows completely unexpected results. First of all, elemental Mg is predicted to undergo several phase transitions induced by pressure: hcp–bcc–fcc–sh. Under ambient conditions, Mg adopts the hcp structure, while bcc–Mg is stable from 50 GPa to 456 GPa, followed by the transition to fcc and the simple hexagonal phase at 456 and 756 GPa, respectively. These results are in excellent agreement with previous studies.[26–28] Unexpectedly, Mg-rich oxides, such as Mg_2O and Mg_3O_2 begin to show very competitive enthalpy of formation at pressures above 100 GPa. However, they are still not stable against decomposition into Mg and MgO, and their crystal structures could
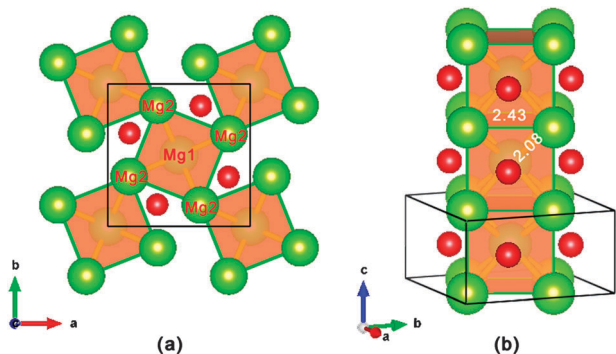
This journal is © the Owner Societies 2013

Phys. Chem. Chem. Phys., 2013, **15**, 7696–7700 | **7697**

Fig. 3 (a) Crystal structures of t-Mg_3O_2 at 500 GPa, space group $P4/mbm$, a = 4.508 Å, c = 2.367 Å, Mg1(0.3494, 0.1506, 0.5); Mg2(0, 0, 0); O(0.8468, 0.6532, 0). (b) View, highlighting the 1D-column of body-centered Mg-cubes.

be thought of as a combination of blocks of Mg and B1-MgO. This situation qualitatively changes at 500 GPa, where we find that Mg_3O_2 becomes thermodynamically stable. This new stable (t-Mg_3O_2) phase has a very unusual tetragonal structure with the space group $P4/mbm$.

This crystal structure can be viewed as a packing of O atoms and 1D-columns of almost perfect body-centered Mg-cubes. As shown in Fig. 3, there are two types of Mg atoms in the unit cell, Mg1 and Mg2. Here, Mg2 atoms form the cubes, merged into vertical columns and filled by Mg1 atoms. Within the cubic columns, one can notice empty $(Mg1)_2(Mg2)_4$ clusters with the shape of flattened octahedra, with Mg–Mg distances ranging from 2.08 Å (Mg1–Mg2) to 2.43 Å (Mg2–Mg2). The coordination environments are quite different: each Mg1 is bonded to two Mg1 atoms and eight Mg2 atoms, while each Mg2 atom is bonded to six O atoms (trigonal prismatic coordination). Oxygen atoms in t-Mg_3O_2 are coordinated by eight Mg2 atoms.

3.3 Possible role of the new compounds in planetary interiors

What are the implications of these two compounds for planetary sciences? High pressures, required for their stability, are within the range corresponding to deep planetary interiors. In terrestrial planetary interiors, reducing conditions dominate, related to the excess of metallic iron. However, given the diversity of planetary bodies one can imagine that on some planets strongly oxidized environments t-MgO_2 can be present at depths corresponding to the pressure of 116 GPa (in the Earth this corresponds to depths greater than 2600 km). Mg_3O_2 is stable under the more usual planetary interior reducing conditions and at pressures above 500 GPa, characteristic of the interiors of giant planets. There, it can coexist in equilibrium with Fe (but probably not with FeO, according to our DFT and DFT + U calculations of the reaction FeO + Mg_3O_2 → Fe + 3MgO). According to our calculations (Fig. 4), Mg_3O_2 can only be stable at temperatures below 1800 K, which is too cold for deep interiors of giant planets; however, impurities and entropy effects stemming from defects and disorder may extend its stability field into planetary temperatures. Exotic compounds MgO_2 and Mg_3O_2, in addition to their general chemical interest, can be important planet-forming minerals in some exotic planets.
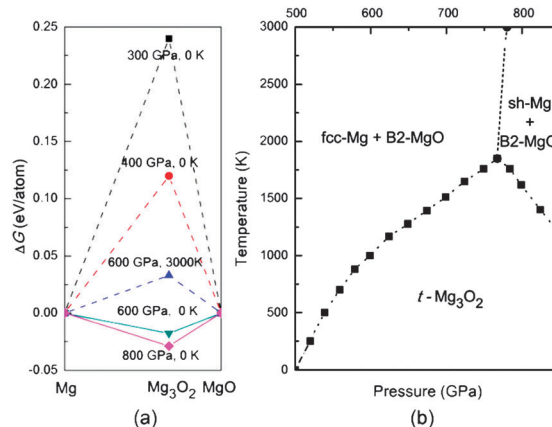

Fig. 4 (a) Convex hull for the Mg–MgO system at high pressures. (b) Predicted P–T stability field and decomposition conditions of t-Mg_3O_2.

4 Electronic structure and chemical bonding

Phonon calculations for Mg_3O_2 and MgO_2 at pressures of their stability show that no imaginary phonon frequencies exist throughout the Brillouin zone, suggesting that these structures are dynamically stable. Together with our calculated thermodynamic functions, this suggests thermodynamic stability of these compounds. What stabilizes these exotic magnesium oxides at high pressure? To answer this question, we analyzed the electronic structure and chemical bonding for these compounds.

Electron Localization Function (ELF) gives information about the bonding character and valence electron configuration of atoms in a compound.[29] The ELF pictures show asymmetry of the Mg–O bonds, indicating significantly ionic character of bonding. As shown in Fig. 5a, valence electrons in t-MgO_2 are mainly concentrated around O atoms. Charge transfer was also investigated on the basis of the electron density using Bader analysis.[30,31] In t-MgO_2, the net charge on Mg is +1.747 e, indicating the nearly complete transfer of valence electrons of Mg to O atoms (just like Mg in MgO: Bader charges are +1.737 e at 0 GPa and +1.675 e at 600). Each O has almost 7 valence electrons (6.873 e), thus with the formation of a singly bonded O–O dumbbell the octet rule is fulfilled. Each O–O dumbbell can be viewed as a peroxide-ion $[O–O]^{2-}$ with a closed-shell electronic configuration.

The ELF distribution in t-Mg_3O_2 (Fig. 5b) also shows strong charge transfer from Mg to O. However, we surprisingly found a very strong interstitial ELF maximum (ELF = 0.97) located in the center of the Mg-octahedron (Fig. 5c). To obtain more insight, we performed Bader analysis. The resulting charges are +1.592 e for Mg1, +1.687 e for Mg2, −1.817 e for O, and −1.311 e for the interstitial electron density maximum. Such a strong interstitial electronic accumulation requires an explanation. The electronic structure (Fig. 5e) exhibits intriguingly high occupancy of Mg-p,d-orbitals with overlapping energy ranges, which implies a strong Mg 3p–3d hybridization. At high pressure, strong interstitial electron localization was found in alkali and alkaline-earth elements; for instance, sodium becomes a transparent
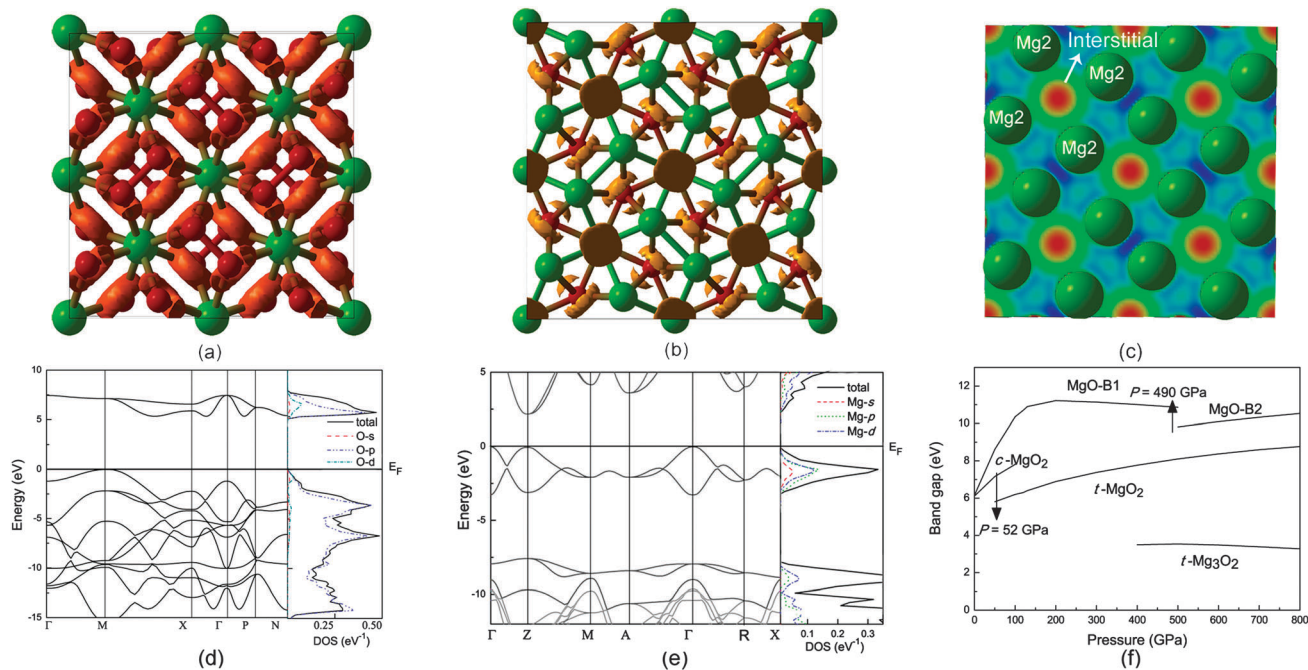
Fig. 5 ELF isosurfaces (ELF = 0.83) in (a) t-MgO$_2$ structure; (b) t-Mg$_3$O$_2$ structure at 500 GPa. (c) Charge density distribution of t-Mg$_3$O$_2$ along the c axis. Band structure and partial densities of states for (d) t-tetragonal MgO$_2$ and (e) t-Mg$_3$O$_2$. (f) Calculated HSE band gaps as a function of pressure for various Mg–O compounds.

insulator due to strong core–core orbital overlap.[32] As a measure of size of the core region we use the Mg^{2+} ionic radius (0.72 Å (ref. 33)), while the size of the valence electronic cloud is represented by the 3s orbital radius (1.28 Å (ref. 34)). In Mg$_3$O$_2$, Mg–Mg contacts at 500 GPa (2.08 Å for Mg1–Mg2, 2.37 Å for Mg1–Mg1 and 2.43 Å for Mg2–Mg2) are only shorter than the sum of valence orbital radii, but longer than the distance at which strong core–valence overlap occurs between neighboring Mg atoms (0.72 + 1.28 Å = 2.00 Å). Thus, the main reason for strong interstitial electronic localization is the formation of strong multicenter covalent bonds between Mg atoms; the interatomic core–valence expulsion (which begins at distances slightly longer than the sum of core and valence radii, 2.00 Å in this case, and increases as the distance decreases) could also play some role for valence electron localization. Strong Mg–Mg covalent bonding is not normally observed; the valence shell of the Mg atom only has a filled 3s^2 orbital, a configuration unfavorable for strong or directional bonding. Under pressure, the electronic structure of the Mg atom changes (p- and d-levels become significantly populated), and strong covalent bonding and electronic localization appear as a result of p–d hybridization. There is another way to describe chemical bonding in this unusual compound. We remind that Mg$_3$O$_2$ is anion-deficient compared with MgO; the extra localized electrons in Mg octahedron interstitial play the role of anions, screening Mg atoms from each other. These two descriptions are complementary.

We also employed HSE hybrid functional as implemented in the VASP code[35] to estimate band gaps for these compounds; hybrid functionals are known to produce much more accurate band gaps than standard semilocal density functionals.

Compared with MgO, which is a wide gap insulator (HSE band gap of 9.82 eV at 500 GPa – see Fig. 5f), t-Mg$_3$O$_2$ is predicted to have a much narrower band gap of 3.54 eV, while the band gap of t-MgO$_2$ at 500 GPa is 8.11 eV. While MgO remains a wide-gap insulator in a very wide pressure range, the band gap can be decreased by changing the stoichiometry of a magnesium oxide.

5 Conclusions

In summary, we performed a systematic search for possible stoichiometries in the Mg–O system at pressures up to 850 GPa. Other than the well-known compound, MgO, we found that two more stoichiometries (MgO$_2$ and Mg$_3$O$_2$) become thermodynamically stable at pressures above 116 GPa and 500 GPa, respectively. Our analysis reveals that bonding in both insulating t-MgO$_2$ and semiconducting t-Mg$_3$O$_2$ exhibits significantly ionic character. MgO$_2$ is stabilized by the formation of the peroxide [O–O]$^{2-}$ anion, while the strong electron localization in the Mg octahedron plays the role of an additional anion and makes the anion-deficient compound Mg$_3$O$_2$ stable. These two compounds might exist in interiors of other planets, and are thus potentially important for our fundamental understanding of the universe – in addition to presenting new striking chemical phenomena.

Acknowledgements

References

1 T. S. Duffy, R. J. Hemley and H.-k. Mao, *Phys. Rev. Lett.*, 1995, **74**, 1371–1374.

2 M. J. Mehl, R. E. Cohen and H. Krakauer, *J. Geophys. Res., [Solid Earth Planets]*, 1988, **93**, 8009–8022.

3 A. R. Oganov, M. J. Gillan and G. D. Price, *J. Chem. Phys.*, 2003, **118**, 10174–10182.

4 A. B. Belonoshko, S. Arapan, R. Martonak and A. Rosengren, *Phys. Rev. B: Condens. Matter Mater. Phys.*, 2010, **81**, 054110.

5 K. Umemoto, R. M. Wentzcovitch and P. B. Allen, *Science*, 2006, **311**, 983–986.

6 H. Wriedt, *J. Phase Equilib.*, 1987, **8**, 227–233.

7 J. M. Recio and R. Pandey, *Phys. Rev. A: At., Mol., Opt. Phys.*, 1993, **47**, 2075–2082.

8 Z. Wang, J. Bentley, E. Kenik, L. Horton and R. McKee, *Surf. Sci.*, 1992, **273**, 88–108.

9 Q. Zhu, D. Jung, A. R. Oganov, C. Glass, C. Gatti and A. O. Lyakhov, *Nat. Chem.*, 2013, **5**, 61–65.

10 E. Zurek, R. Hoffmann, N. W. Ashcroft, A. R. Oganov and A. O. Lyakhov, *Proc. Natl. Aca. Sci. U. S. A.*, 2009, **106**, 17640–17643.

11 R. T. Howie, O. Narygina, C. L. Guillaume, S. Evans and E. Gregoryanz, *Phys. Rev. B: Condens. Matter Mater. Phys.*, 2012, **86**, 064108.

12 W. Zhang, A. R. Oganov, A. F. Goncharov, Q. Zhu, S. E. Boulfelfel, A. O. Lyakhov, M. Somayazulu and V. B. Prakapenka, *arXiv preprint arXiv:1211.3644*, 2012.

13 A. R. Oganov and C. W. Glass, *J. Chem. Phys.*, 2006, **124**, 244704.

14 A. O. Lyakhov, A. R. Oganov and M. Valle, *Comput. Phys. Commun.*, 2010, **181**, 1623–1632.

15 A. O. Lyakhov, A. R. Oganov, H. T. Stokes and Q. Zhu, *Comput. Phys. Commun.*, 2013, **184**, 1172–1182.

16 A. R. Oganov, A. O. Lyakhov and M. Valle, *Acc. Chem. Res.*, 2011, **44**, 227–237.

17 J. P. Perdew, K. Burke and M. Ernzerhof, *Phys. Rev. Lett.*, 1996, **77**, 3865–3868.

18 G. Kresse and J. Furthmüller, *Phys. Rev. B: Condens. Matter Mater. Phys.*, 1996, **54**, 11169–11186.

19 P. E. Blöchl, *Phys. Rev. B: Condens. Matter Mater. Phys.*, 1994, **50**, 17953–17979.

20 A. Togo, F. Oba and I. Tanaka, *Phys. Rev. B: Condens. Matter Mater. Phys.*, 2008, **78**, 134106.

21 N.-G. Vannerberg, in *Peroxides, Superoxides, and Ozonides of the Metals of Groups Ia, IIa, and IIb*, John Wiley Sons, Inc., 2007, pp. 125–197.

22 S. C. Abrahams and J. Kalnajs, *Acta Crystallogr.*, 1954, **7**, 838–842.

23 I. Efthimiopoulos, K. Kunc, S. Karmakar, K. Syassen, M. Hanfland and G. Vajenine, *Phys. Rev. B: Condens. Matter Mater. Phys.*, 2010, **82**, 134125.

24 N. Vannerberg, *Ark. Kemi*, 1959, **14**, 99–105.

25 Y. Ma, A. R. Oganov and C. W. Glass, *Phys. Rev. B: Condens. Matter Mater. Phys.*, 2007, **76**, 064101.

26 H. Olijnyk and W. B. Holzapfel, *Phys. Rev. B: Condens. Matter Mater. Phys.*, 1985, **31**, 4682–4683.

27 R. M. Wentzcovitch and M. L. Cohen, *Phys. Rev. B: Condens. Matter Mater. Phys.*, 1988, **37**, 5571–5576.

28 P. Li, G. Gao, Y. Wang and Y. Ma, *J. Phys. Chem. C*, 2010, **114**, 21745–21749.

29 A. D. Becke and K. E. Edgecombe, *J. Chem. Phys.*, 1990, **92**, 5397–5403.

30 R. F. W. Bader, *Atoms in Molecules – A Quantum Theory*, Oxford University Press, 1990.

31 G. Henkelman, A. Arnaldsson and H. Jonsson, *Comput. Mater. Sci.*, 2006, **36**, 354–360.

32 Y. Ma, M. I. Eremets, A. R. Oganov, Y. Xie, I. Trojan, S. Medvedev, A. O. Lyakhov, M. Valle and V. Prakapenka, *Nature*, 2009, **458**, 182–185.

33 R. D. Shannon and C. T. Prewitt, *Acta Crystallogr., Sect. B: Struct. Crystallogr. Cryst. Chem.*, 1969, **25**, 925–946.

34 J. T. Waber and D. T. Cromer, *J. Chem. Phys.*, 1965, **42**, 4116–4123.

35 A. V. Krukau, O. A. Vydrov, A. F. Izmaylov and G. E. Scuseria, *J. Chem. Phys.*, 2006, **125**, 224106.